

Abstract

Travelling standing wave (TSW) sometimes called optical conveyor belt (OCB) can be used to deliver Brownian particles in one dimension by a controlled way. Thermal noise causes that the speed of the particle delivery is not generally the same as the speed of the TSW because the particle hops between neighboring stable equilibrium positions (optical traps). These hops slow down the speed of the particle delivery and two limiting cases can be distinguished. *Brownian surfer* is obtained if the standing wave travels slowly and provides deep enough potential wells so that the particle is tightly coupled to the well and “surfs along with the potential wave”. If the velocity of the TSW is high and the potential well is shallower, the particle - *Brownian swimmer* is not dragged by the wave in motion and behaves more like a swimmer afloat on the surface of the ocean.

Theoretical description

We assume that a microbead is located in a periodic array of optical traps travelling with constant velocity v . The random motion of the bead is described by stochastic Langevin equation

$$\gamma \dot{x}(t) = -U'(x(t)) - \gamma v + \xi(t), \quad (1)$$

where γ is the Stokes coefficient, $x(t)$ is the particle coordinate and $U(x)$ is the periodic potential with the period L . Since the particle is very light and moves in viscous medium, its overdamped motion is supposed and therefore the inertial term $m\ddot{x}$ is omitted. An interference of two counterpropagating plane waves creates a potential profile $U(x) = \Delta U/2 \cos(4\pi n_{\text{ext}}x/\lambda)$, where ΔU is the potential well depth, n_{ext} is the refractive index of the surrounding medium (water) and λ is the vacuum wavelength of interfering light waves.

Let us further consider a statistical ensemble of the stochastic processes belonging to independent realizations of random fluctuations $\xi(t)$. The corresponding probability density $P(x, t)$ in space x and time t describes the distribution of Brownian particles. The time evolution of $P(x, t)$ is given by Fokker-Planck equation (FPE)

$$\frac{\partial}{\partial t} P(x, t) = \frac{\partial}{\partial x} \left\{ \frac{U'(x)}{\eta} P(x, t) \right\} + \frac{k_B T}{\eta} \frac{\partial^2}{\partial x^2} P(x, t), \quad (2)$$

Particle current $\langle \dot{x} \rangle$ is the quantity of the foremost interest in the context of the transport in the periodic potentials. It is defined as the time-dependent ensemble average over the velocities. To solve FPE (2) it is useful to use a reduced probability density \tilde{P} that enables to solve FPE only over one period L with periodic boundary conditions. For physical reasons we expect that $\tilde{P}(x, t)$ approaches a steady state $\tilde{P}^{\text{st}}(x)$ in the long time limit $t \rightarrow \infty$. The reduced probability then fulfills

$$\tilde{P}^{\text{st}} = \mathcal{N} \frac{\gamma}{k_B T} e^{-U_{\text{eff}}(x)/k_B T} \int_x^{x+L} dy e^{U_{\text{eff}}(y)/k_B T}, \quad (3)$$

where \mathcal{N} is the normalization constant and $U_{\text{eff}}(x) = U(x) + \gamma vx$. For the particle current, or the mean particle velocity can be obtained

$$\langle \dot{x} \rangle = v - \frac{Lk_B T}{\gamma} \frac{[\exp(\gamma v L/k_B T) - 1]}{\int_0^L dx \int_x^{x+L} dy \exp\left\{\frac{U(y) - U(x) + (y-x)\gamma v}{k_B T}\right\}}. \quad (4)$$

The particle current $\langle \dot{x} \rangle$ is *always smaller* than the velocity of travelling potential v but it has always the same sign as v .

For high velocities the particle does not feel the presence of the traveling potential and behaves like a *Brownian swimmer*. For small velocities v the particle is tightly coupled to one potential well and so follows the potential movement as the *Brownian surfer*. The current $\langle \dot{x} \rangle$ tends to zero for both very small and very large speeds v and therefore there has to exist an optimum OCB velocity v that provides the maximal particle speed. Figure 1 shows an example of the mean velocity of the bead 520 nm in diameter moving in water. This mean velocity was calculated for different traveling potential speeds v and different heights of the potential barriers ΔU .

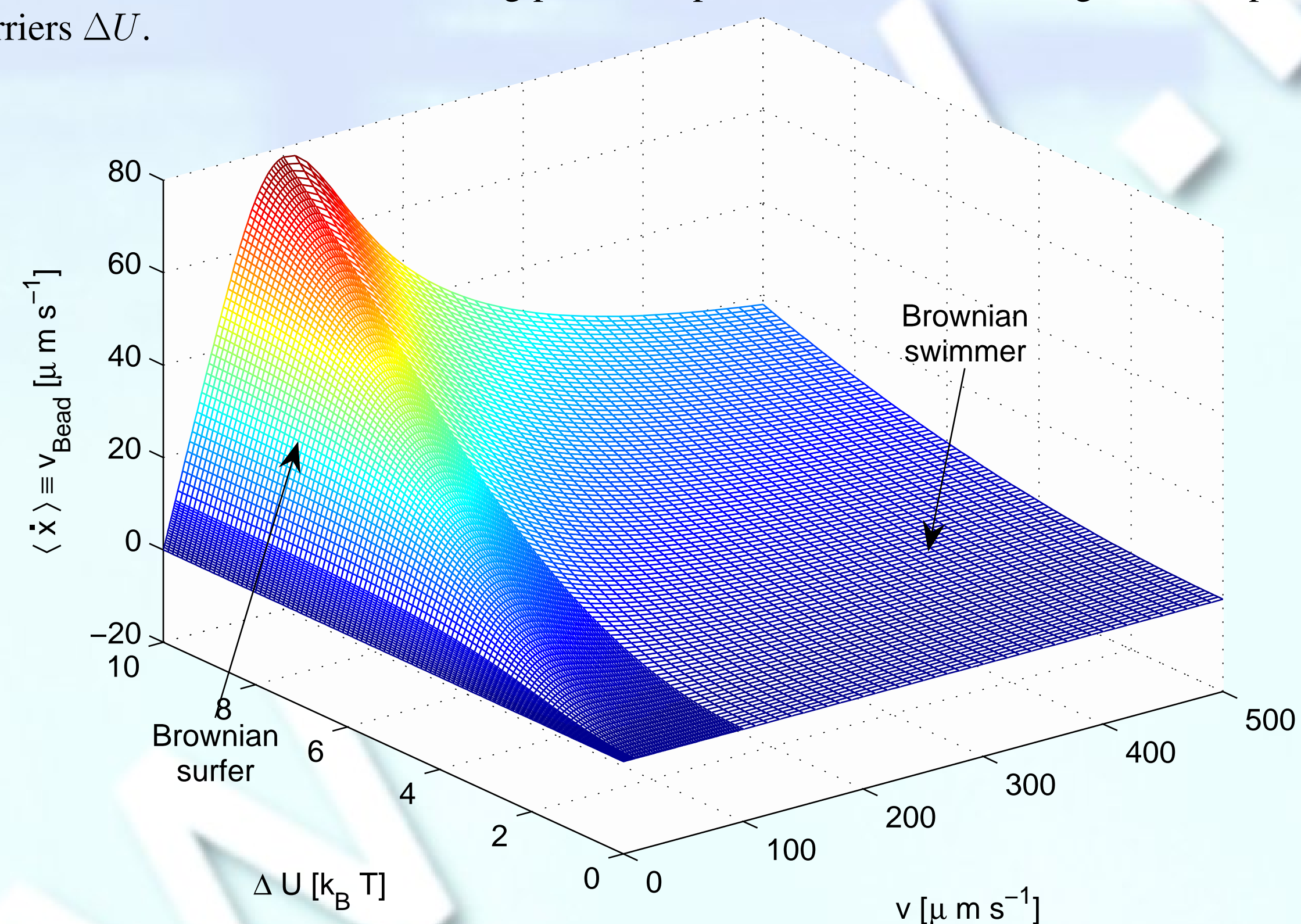


Figure 1. The mean velocity of a polystyrene bead of 520 nm in diameter placed to the traveling periodic potential. The limiting regions of the Brownian surfer (on the left) and the Brownian swimmer (on the right) are marked. The combinations of the wave velocity v and potential well depths ΔU can be found so that the particle velocity will be maximized.

Illustration of surfer and swimmer cases

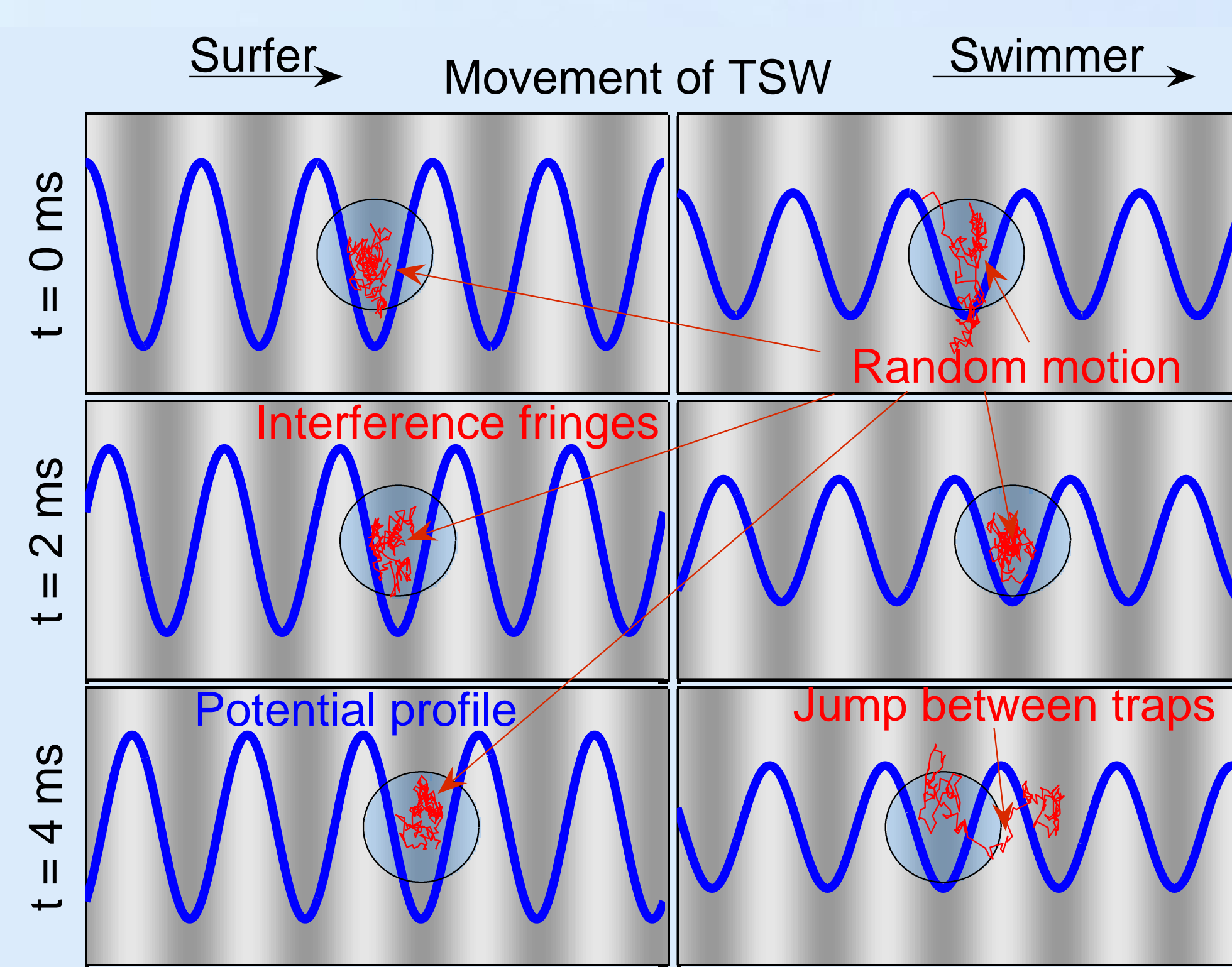


Figure 2. TSW moves with velocities $20 \mu\text{ms}^{-1}$, left column, and $40 \mu\text{ms}^{-1}$, right column. Trap depths are $\Delta U = 5 k_B T$ in slower TSW and $\Delta U = 3.3 k_B T$ in faster TSW. Interference fringes and potential profile are shown in 3 different times. The position of bead is symbolically shown by ping circle and the random motion of bead between frames is shown by red line. The slower TSW demonstrates surfer case with bead still localized in one optical trap. The faster case shows swimmer case with jumps between neighboring optical traps.

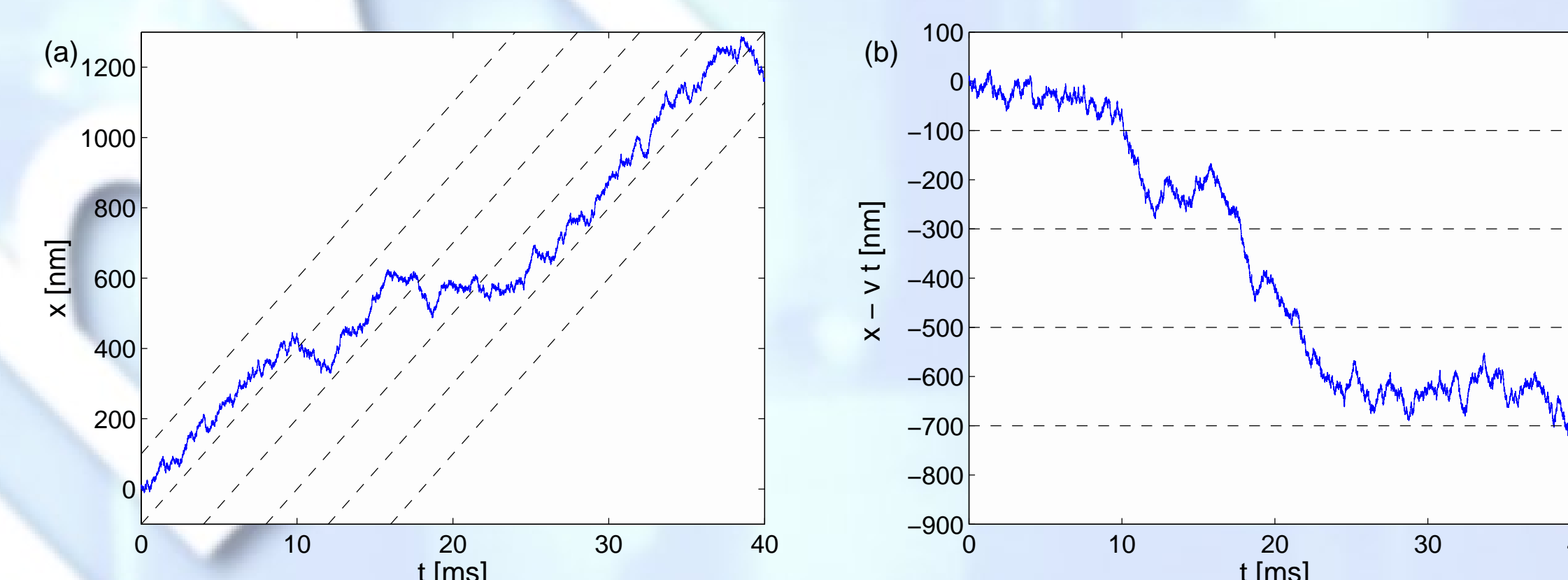


Figure 3. Monte-Carlo simulation of the bead positions in the traveling standing wave (TSW) with respect to the fixed coordinate system (a – left) and to the coordinate system traveling with standing wave (b – right). The following parameters were considered: $v = 50 \mu\text{ms}^{-1}$, $\Delta U = 5 k_B T$ and bead diameter $d = 520 \text{ nm}$. The dashed lines show borders between neighboring optical traps. The average velocity of the bead obtained from the MC simulation or Eq. (4) in this interval is $28.83 \mu\text{ms}^{-1}$ or $28.77 \mu\text{ms}^{-1}$, respectively.

Experimental results

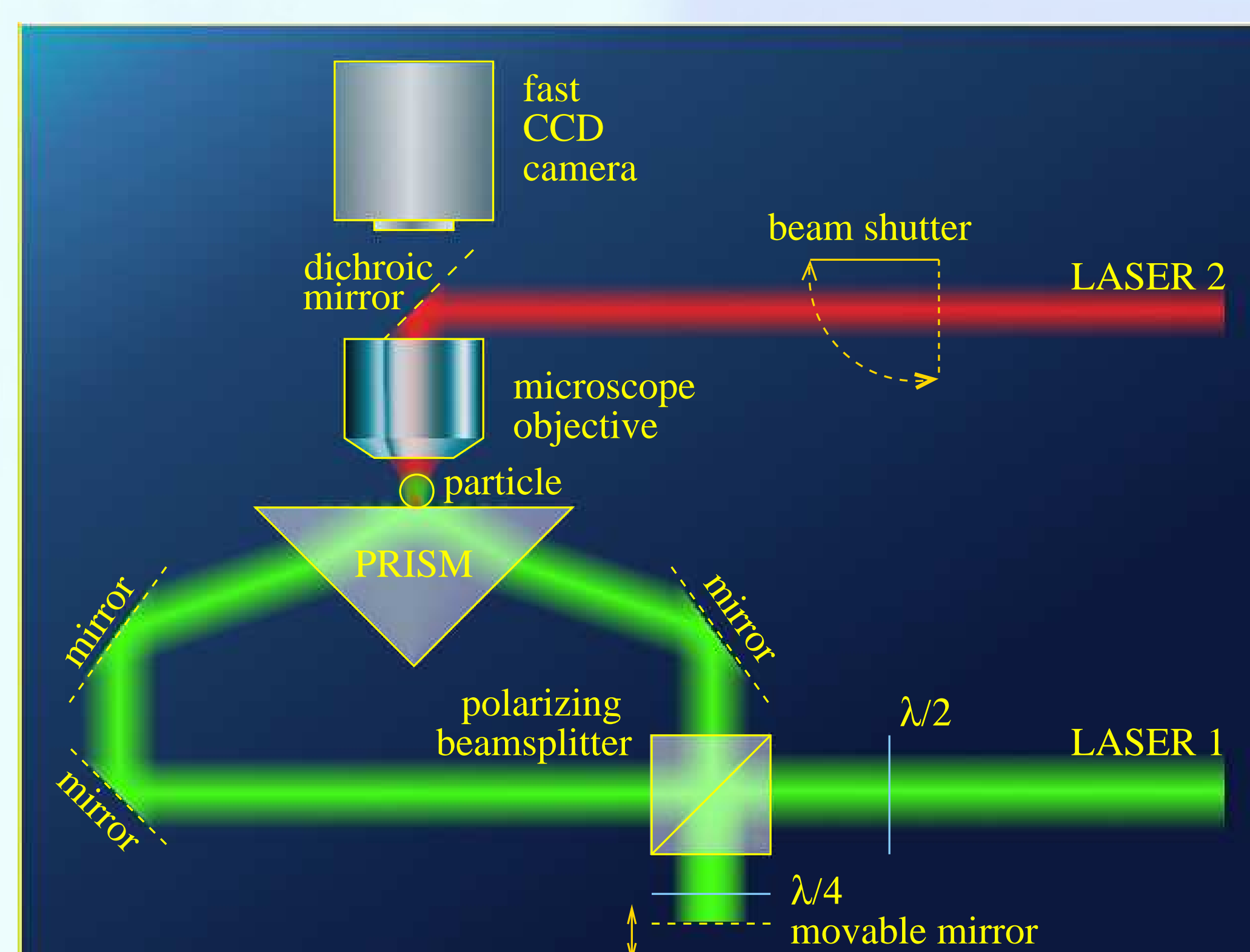


Figure 4. Schematic diagram of experimental setup.

Conclusions

- The average bead velocity was derived theoretically by means of Fokker-Planck equation. The conditions for “surfer” and “swimmer” cases were discussed.
- The behavior of bead in motional standing wave was studied by Monte-Carlo simulations in one dimension. The simulations validated theoretical predictions.
- Evanescent wave conveyor belt was used to compare theoretical results with experiment. Some deviations indicates that the theoretical model should be extended to more dimensions to include also particle movement perpendicular to the surface.

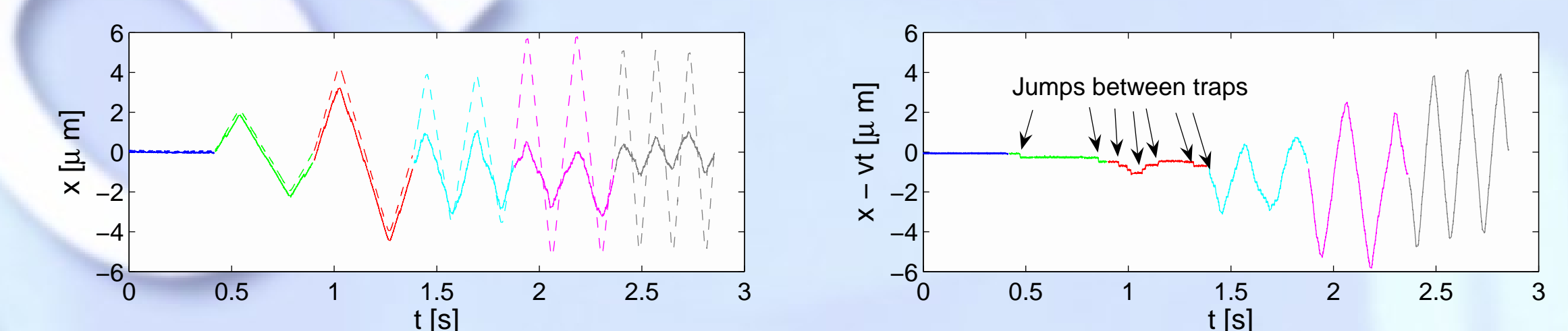


Figure 5. Record of bead positions while TSW moves with different speeds. Top: positions of the bead during the movement (solid lines) and the displacement of the original bead position at $t = 0$ corresponding to the motion of the standing wave (dashed sawtooth curve). Bottom: the position of the bead with respect to TSW. Different colors show the different TSW speeds.

Processing the same data as shown in Fig. 5 we obtained the average speeds of the confined bead and also the speed of the TSW. They were compared to the theoretical values from Eq. (4). The theoretical green curve in Eq. (4) was fitted to the experimental data using the trap depth ΔU as the only free parameter. The slowest TSW velocity provided optimal conditions for the existence of Brownian surfer. Faster TSW motion has not reached the conditions for Brownian swimmer and the bead was dragged by the TSW with smaller relative speed.

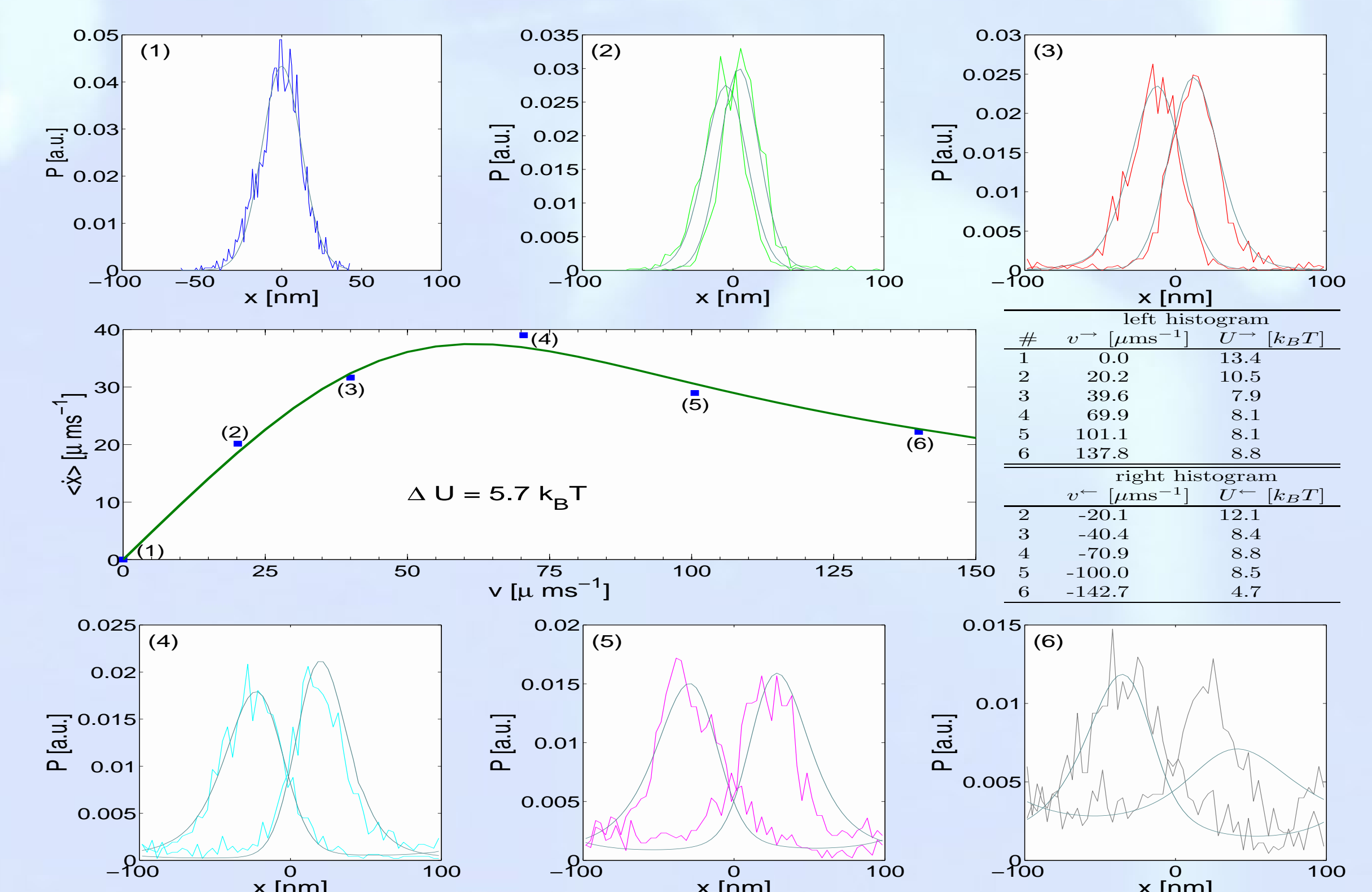


Figure 6. Center: The average velocities of the bead placed in TSW moving with different speeds. The squares show experimental data and the curve is a fit by Eq. (4). The trap depth was the only fitting parameter and its following value was found $\Delta U = 5.7 \pm 0.4 k_B T$. For each point the histograms of bead position with respect to the standing wave and fit by the reduced probability (3) are shown. The fitted parameter in histograms is ΔU while velocity v is taken from Fig. 5. The values of v and ΔU fitted from histograms are in table on the right.

Equation (3) can be used to determine parameters of the motional system such as trap depth, bead mean velocity or the liquid viscosity at place of the bead. The trap depths calculated from histograms if Fig. 6 are different from the stationary trap depth (left bottom histogram). The differences are caused by the fact that our model is only one dimensional while the experimental setup is 3 dimensional. Also the presence of the boundary and the changes of the viscosity close to the surface are not taken into account. Yet the model presented here describes problem well and the predicted results are in coincidence with experiment.

References

- H. Risken, *The Fokker-Planck Equation*, Springer-Verlag, Berlin, 1996.
- P. Reimann, “Brownian motors: noisy transport far from equilibrium,” *Physics Reports* **361**, pp. 57–265, 2002.
- M. Šiler, T. Čížmár, M. Šerý, and P. Zemánek, “Optical forces generated by evanescent standing waves and their usage for sub-micron particle delivery,” *Appl. Phys. B* **84**, pp. 157–165, 2006.
- T. Čížmár, M. Šiler, M. Šerý, P. Zemánek, V. Garcés-Chávez, and K. Dholakia, “Optical sorting and detection of sub-micron objects in a motional standing wave,” *Phys. Rev. B* **74**, pp. 035105, 2006.

Acknowledgments

This work was partially supported by the Institutional Research Plan of the Institute of Scientific Instruments (AV0Z20650511), Grant Agency of the Academy of Sciences (IAA1065203), European Commission via 6FP NEST ADVENTURE Activity (ATOM3D, project No. 508952), and Ministry of Education, Youth, and Sports of the Czech Republic (project No. LC06007).